Technique for active stabilization of the relative phase between seed and pump in an optical parametric oscillator

Simone Cialdi,[*] Edoardo Suerra,[†] Matteo G. A. Paris,[‡] and Stefano Olivares[§]
Dipartimento di Fisica "Aldo Pontremoli," Università degli Studi di Milano, via Celoria 16, I-20133 Milan, Italy and Istituto Nazionale di Fisica Nucleare, Sezione di Milano, I-20133 Milan, Italy

(Received 13 July 2021; accepted 20 October 2021; published 12 November 2021)

We design and demonstrate a technique for the active stabilization of the relative phase between seed and pump in an optical parametric oscillator (OPO). We show that two error signals for the stabilization of the OPO frequency, based on Pound-Drever-Hall (PDH), and of the seed-pump relative phase can be obtained just from the reflected beam of the OPO cavity, without the necessity of two different modulation and demodulation stages. We also analyze the effect of the pump in the cavity stabilization for different seed-pump relative phase configurations, resulting in an offset in the PDH error signal, which has to be compensated. Finally, an application of our technique in the reliable generation of squeezed coherent states is presented.

DOI: 10.1103/PhysRevA.104.053706

I. INTRODUCTION

"Squeezing" is a fundamental resource in continuous-variable quantum information science [1] and in gravitational-wave detection [2]. For these and other applications a key ingredient is the use of squeezed states, which are commonly generated via an optical parametric oscillator (OPO) [3–7]. The basic elements of an OPO are an optical cavity (the resonator) with a nonlinear crystal. Whereas the cavity allows us to select a particular frequency of the field, the crystal, suitably "pumped" by an input laser beam (the "pump"), provides the "squeezing." The generated states can be further manipulated by changing their coherent amplitude and phase. However, this requires using a "seed," namely, a coherent state with a well-determined complex amplitude, that interacts with the nonlinear crystal, leading to the so-called squeezed coherent states. Mechanical vibrations largely affect this kind of device, forcing the use of active stabilization. Different techniques have been developed to this aim: the Pound-Drever-Hall (PDH) technique [8], homodyne locking [9], the modulation-free technique [10], and tilt locking [11], just to mention the most commonly used. Moreover, also the relative phase between the seed and the pump used for squeezing has to be stabilized. This has been performed using modulation techniques such as in Ref. [12,13], or in GEO600 [14] or through the weak pump depletion (WPD) technique [15].

Here we present the theoretical basis and the demonstration of an innovative technique for the seed-pump relative phase stabilization of an OPO with an application to the generation of squeezed coherent states. With respect to modulation techniques [12], ours allows us to obtain two different error signals directly from the reflected beam. The first signal is for the OPO frequency stabilization and it is based on the PDH technique, but taking into account the presence of the pumped nonlinear crystal inside the cavity. In fact, since the standard PDH technique is based on an empty cavity, here we first have to derive the theoretical model to include the effect of the crystal. The other signal is for the seed-pump phase stabilization and does not require an additional modulation and demodulation stage. Thanks to this method, we do not need a detection system for the pump, that is instead necessary, for instance, in the WPD technique [15]. Remarkably, our approach allows us to retrieve relevant information about the dynamics of the error signal and to show how the pump affects the PDH error signal and how to correct this error signal.

The article is structured as follows: In Sec. II the technique is theoretically described, taking into account the presence of the crystal inside the cavity. The setup for the implementation and the experimental results are shown in Sec. III. Our pump-seed stabilization technique is applied in Sec. IV to generate squeezed coherent states. Finally, we draw some concluding remarks in Sec. V.

II. THEORY

As in the case of the usual PDH stabilization technique, our approach is based on the detection of the beam reflected off the cavity but in the presence of a nonlinear crystal in it, that is also pumped to produce squeezing. It is worth noting that the seed (at 1064 nm in our experiment, see Sec. III) and the pump (at 532 nm) have different frequencies. Therefore, in this Section we develop a proper theoretical model to describe a two-mirror cavity with a pumped nonlinear crystal inside, namely, the OPO.

As sketched in Fig. 1, the mirror M_1, with reflectivity R_1, serves as the input coupler for the seed $E_{\rm in}$, while the mirror M_2, with reflectivity R_2, acts as the input coupler for the pump

[*]simone.cialdi@mi.infn.it
[†]edoardo.suerra@unimi.it
[‡]matteo.paris@fisica.unimi.it
[§]stefano.olivares@fisica.unimi.it

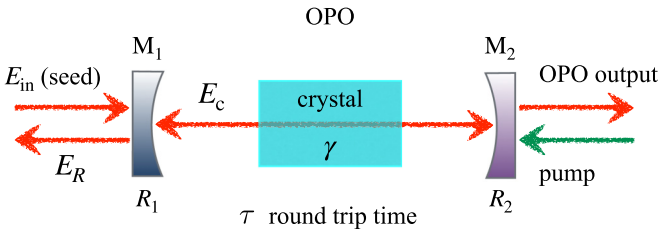

FIG. 1. Scheme of the OPO with the main elements. See text for details.

and as the output coupler for the OPO field. The aim is now to obtain the amplitude of the reflected field E_R as a function of the cavity frequency ν, the crystal nonlinearity γ, and the pump phase ϕ_p.

If the OPO does not contain the nonlinear crystal, the electric field in the cavity $E_c(t+\tau)$ after a round trip with duration τ can be written as the sum of the field already circulating inside the cavity $E_c(t)$ and the input field E_{in}, that is

$$E_c(t+\tau) = \sqrt{1-R_1}E_{in} + \sqrt{R}e^{i\phi}E_c(t), \tag{1}$$

where $R = R_1R_2(1-\Delta)^2$, Δ is the internal power losses for the single round trip, and $\phi = 2\pi\nu/\Gamma$. Here, $\nu = \nu_{in} - \nu_c$ is the detuning between the input and the cavity frequencies and Γ is the free spectral range of the cavity.

In the presence of the nonlinear crystal inside the cavity, Eq. (1) has to be modified by adding a term accounting for interaction between the light and the crystal. The interaction can be effectively described by introducing a dimensionless complex parameter γ which depends on the nonlinearity of the crystal and on the pump field amplitude and its phase. Assuming a round trip much faster than the intracavity fields dynamics, we can expand $E_c(t+\tau)$ up to the first order in τ, and Eq. (1) leads to

$$\frac{dE_c}{dt}\tau = \sqrt{1-R_1}E_{in} + (\sqrt{R}e^{i\phi} - 1)E_c + i\gamma E_c^*. \tag{2}$$

The fact that here appears the complex conjugate of the cavity field, E_c^*, directly follows from energy conservation in the nonlinear interaction [16]. Therefore, at equilibrium we have

$$(1-\sqrt{R}e^{i\phi})E_c - i\gamma E_c^* = \sqrt{1-R_1}E_{in}. \tag{3}$$

Without loss of generality, from now on we can set $E_{in} = 1$ (or, equivalently, we are measuring the fields in units of the input field) and, thus, the phases of the involved fields are relative to the phase of the input field. From Eq. (3) we obtain

$$E_c = \sqrt{1-R_1}\,\frac{1-\sqrt{R}e^{-i\phi} + i|\gamma|e^{i\phi_p}}{1+R-2\sqrt{R}\cos\phi - |\gamma|^2}, \tag{4}$$

where $\gamma = |\gamma|e^{i\phi_p}$, ϕ_p being the pump phase relative to the seed phase. It is worth noting that E_c can be continuously modulated from an amplification regime ($\phi_p = -\pi/2$) to a de-amplification regime ($\phi_p = \pi/2$). As a matter of fact, if $\gamma \to 0$ we find the usual equation of a two-mirror cavity without the nonlinear crystal, as one may expect.

The actual value of $|\gamma|$ can be obtained experimentally and we can relate it to a measurable quantity. In fact, one has

$$G = \frac{G_+}{G_-} = \left|\frac{1+\delta}{1-\delta}\right|^2, \tag{5}$$

where $\delta = |\gamma|/(1-\sqrt{R}e^{i\phi})$ and G_+ and G_- are the power of E_c in the amplification and de-amplification regime, respectively. Since the OPO output (see Fig. 1) is clearly proportional to E_c, then G can be measured by monitoring the output power in the two regimes.

Now, we turn our attention to the reflected beam E_R (see Fig. 1), since it will be used to obtain two different error signals for the stabilization of the OPO frequency and the stabilization of the seed-pump relative phase. The reflected beam E_R is the sum of the field directly reflected from the input coupler, with an additive π phase, and the transmitted one through M_1, thus it can be written as (we still set $E_{in} = 1$):

$$E_R = -\sqrt{R_1} + \frac{\sqrt{1-R_1}}{\sqrt{R_1}}(\sqrt{R}e^{i\phi}E_c + i|\gamma|e^{i\phi_p}E_c^*). \tag{6}$$

By substituting Eq. (4) into Eq. (6), we explicitly find

$$E_R = \frac{(\sqrt{R}e^{i\phi} - R_1)(1-\sqrt{R}e^{-i\phi})}{\sqrt{R_1}(1+R-2\sqrt{R}\cos\phi - |\gamma|^2)} + \frac{i[(1-R_1)e^{i\phi_p} + |\gamma|]|\gamma|}{\sqrt{R_1}(1+R-2\sqrt{R}\cos\phi - |\gamma|^2)}. \tag{7}$$

Again, if $\gamma \to 0$, then E_R reduces to the usual reflected field without the nonlinear crystal. E_R depends on the detuning between seed frequency and cavity frequency though ϕ, but also on the pump phase ϕ_p.

In Fig. 2 (top and center panels) we plot $|E_c|^2$ and $|E_R|^2$ as functions of the phase ϕ, proportional to the detuning ν, and of the pump phase ϕ_p for realistic values of the other parameters involved (similar to those we shall use in our experiment described in Sec. III). Remarkably, the minimum value of the intensity of the reflected beam, $|E_R^{(min)}|^2$, depends on the pump phase ϕ_p (see Fig. 2, bottom panel). In particular, the minimum and the maximum of $|E_R^{(min)}|^2$ occur in the amplification ($\phi_p = -\pi/2$) and de-amplification ($\phi_p = \pi/2$) regimes, respectively, as shown in the bottom panel of Fig. 2: between these two extremes, $|E_R^{(min)}|^2$ is monotone with respect to ϕ_p and this allows us to retrieve an *error signal* to stabilize the pump phase. Note that, in other cavity configurations, namely, for a different choice of R_1 and R_2, one can find a *minimum* of the reflected field and a *maximum* of the transmitted one, but the effect of the ϕ_p on their actual values is still the same. Therefore, also in this case we can retrieve the error signal by a suitable electronic inversion.

The stabilization of the cavity frequency is performed by the standard PDH technique, where a phase modulation ϕ_m is added to the seed E_{in} at a frequency ν_m [8]. The equation for the normalized error signal is (we recall that $\phi \propto \nu$) [8,17]

$$\epsilon_{PDH} = \mathrm{Im}[E_R(\nu)E_R^*(\nu-\nu_m) - E_R^*(\nu)E_R(\nu+\nu_m)]. \tag{8}$$

Since E_R depends on ϕ_p, the pump phase influences also the PDH error signal (8). This is a very important point and it will be better discussed in Sec. III. Here we just observe that, in the amplification or in the de-amplification regime,

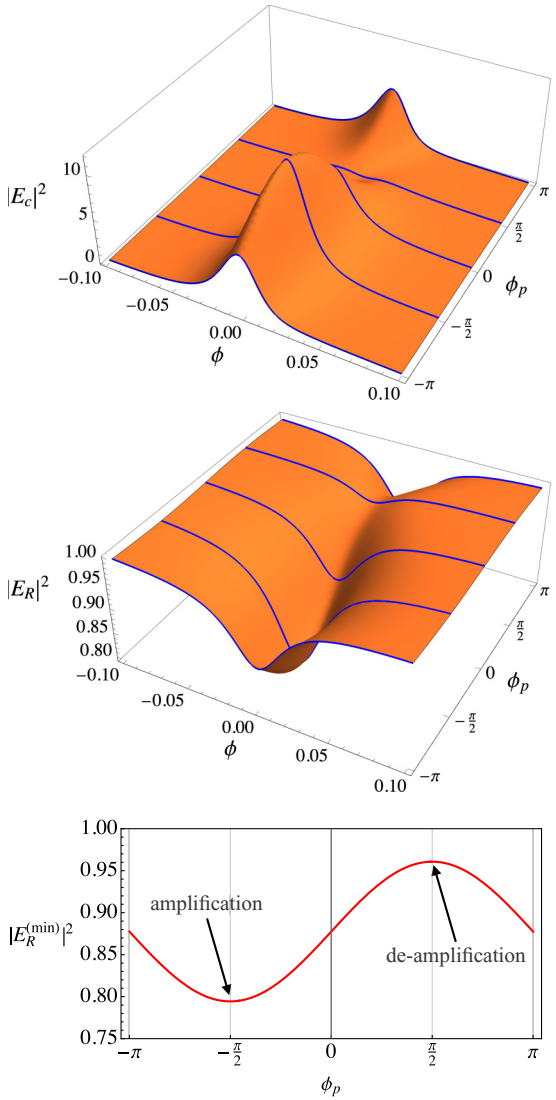

FIG. 2. (top and center) Plots of $|E_c|^2$ and $|E_R|^2$ (dimensionless units) with $E_{in} = 1$ as functions of the phase ϕ, proportional to the detuning ν, and the pump phase ϕ_p. The blue lines refer to the behavior of $|E_c|^2$ and $|E_R|^2$ for a particular choice of the pump phase, from left to right $\phi_p = -\pi$, $-\pi/2$, 0, $\pi/2$, and π. (bottom) Plot of the minimum value $|E_R^{(\min)}|^2$ of the reflected beam amplitude as a function of the pump phase ϕ_p. The other involved parameters have been set to the realistic values $R_1 = 0.999$, $R_2 = 0.9$, $\Delta = 3.0 \times 10^{-3}$, and $|\gamma| = 2.0 \times 10^{-2}$. See text for details.

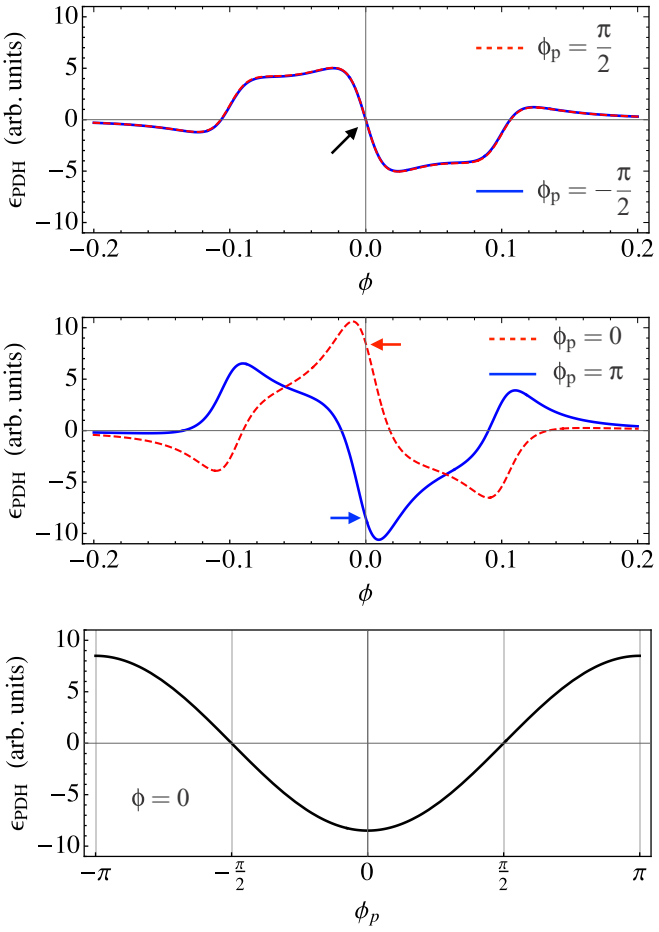

FIG. 3. Plots of the PDH error signal ϵ_{PDH} as a function of $\phi \propto \nu$ for fixed phase modulation $\phi_m = 0.1$ and for different values of the pump phase ϕ_p. (top) In the amplification ($\phi_p = -\pi/2$) or in the de-amplification ($\phi_p = \pi/2$) regime the PDH error signal vanishes at resonance ($\phi = 0$). (center) If $\phi_p \neq \pm\pi/2$ the PDH error signal becomes zero at $\phi \neq 0$: there is an offset (arrows) due to the effect of the pump phase. (bottom) Plot of ϵ_{PDH} as a function of the pump phase ϕ_p at resonance ($\phi = 0$). The other involved parameters have been set to the realistic values $R_1 = 0.999$, $R_2 = 0.9$, $\Delta = 3.0 \times 10^{-3}$, and $|\gamma| = 2.0 \times 10^{-2}$.

the PDH error signal vanishes at resonance, i.e., $\phi = 0$ (top panel of Fig. 3): the field inside the cavity and, in turn, the transmitted beam has a maximum or a minimum when the OPO is resonant with the input field, i.e., $\phi = 0$, only in these two regimes (Fig. 4, top and center panels). More in general, the pump phase ϕ_p may lead to a PDH error signal which is no longer equal to zero at resonance (bottom panel of Fig. 3). To have $\epsilon_{PDH} = 0$ also in this case, the vertical offset has to be compensated. As mentioned, this offset vanishes in the amplification ($\phi_p = -\pi/2$) or in the de-amplification ($\phi_p = \pi/2$) regime: the field inside the cavity and, in turn, the transmitted beam, has a maximum or a minimum when the OPO is resonant with the input field, i.e., $\phi = 0$, only in these two regimes (Fig. 4, top and center panels), otherwise the presence of the pump introduces a detuning of the resonance (Fig. 4, bottom panel). This last effect can be understood by inspecting the analytic expression of the field intensity inside the cavity, namely,

$$|E_c|^2 = \frac{1 - R_1}{1 + R - 2\sqrt{R}\cos\phi - |\gamma|^2} - 2|\gamma|(1 - R_1)\frac{\sin\phi_p - \sqrt{R}\sin(\phi + \phi_p)}{(1 + R - 2\sqrt{R}\cos\phi - |\gamma|^2)^2}. \quad (9)$$

On the one hand, it is clear that the crystal may lead to the amplification process: for instance, if we set $\phi_p = 0$ and $\phi = 0$ (resonance), $|E_c|^2$ increases as $|\gamma|$ grows. On the other hand, the second term of the right-hand side (r.h.s.) in Eq. (9) is responsible for the detuning mentioned above, since it depends on $|\gamma|$ and, in particular, on ϕ_p. In fact, given $\phi_p \neq 0$, the considered term can be positive or negative depending on the

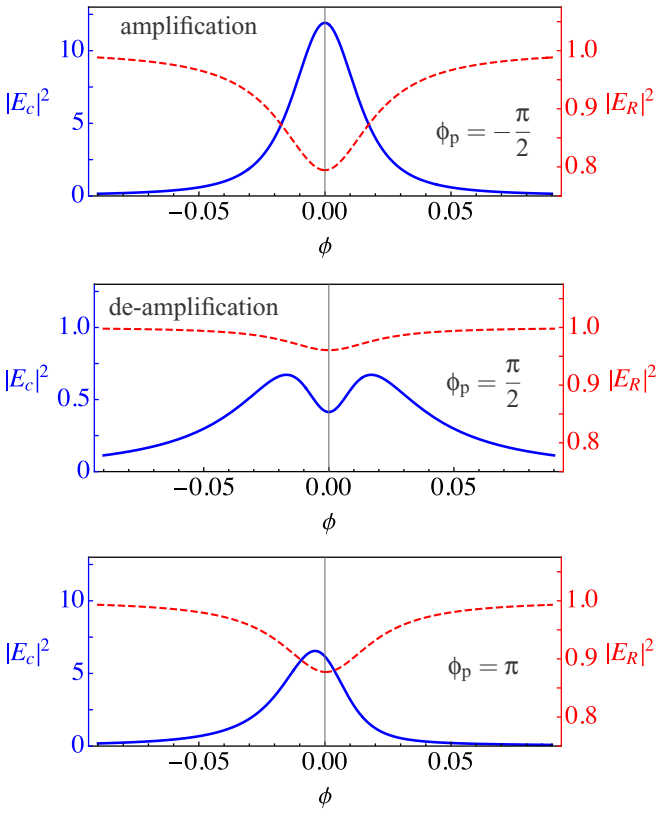

FIG. 4. Plots of $|E_c|^2$ (solid blue lines), proportional to the OPO output, and $|E_R|^2$ (dashed red lines) with $E_{in} = 1$ (dimensionless units) as functions of the phase $\phi \propto \nu$ for different values of the pump phase: (top) $\phi_p = -\pi/2$, amplification regime; (center) $\phi_p = \pi/2$, de-amplification regime; (bottom) $\phi_p = \pi$. The other involved parameters have been set to the realistic values $R_1 = 0.999$, $R_2 = 0.9$, $\Delta = 3.0 \times 10^{-3}$, and $|\gamma| = 2.0 \times 10^{-2}$.

value of $\phi \propto \nu$ and, thus, it eventually results in the detuning of the resonance. In particular, for $\phi_p = \pm\pi/2$ we have

$$|E_c|^2 = \frac{1 - R_1}{1 + R - 2\sqrt{R}\cos\phi - |\gamma|^2} \mp \frac{2|\gamma|(1 - R_1)(1 - \sqrt{R}\cos\phi)}{(1 + R - 2\sqrt{R}\cos\phi - |\gamma|^2)^2}. \quad (10)$$

If we now consider the second term on the r.h.s. in Eq. (10) at resonance ($\phi = 0$), it is clearly positive in the amplification regime ($\phi_p = -\pi/2$) and negative for the de-amplification regime ($\phi_p = \pi/2$). In this last case, we may also have a local minimum at $\phi = 0$ and two maxima at $\phi \neq 0$, as shown in Fig. 5.

For the sake of completeness, in Fig. 6 we plot $|E_c|^2$ and $|E_R|^2$ as functions of the pump phase ϕ_p at resonance, i.e., $\phi \propto \nu = 0$, where $|E_R|^2 = |E_R^{(min)}|^2$ (see the bottom panel of Fig. 2), and for $\phi = 0.02$. Overall, two different offsets have to be kept under control in order to generate two error signals: one for the OPO stabilization, obtained by centering the PDH error signal in zero (top panel of Fig. 7), and one for seed-pump stabilizer (SPS), retrieved by fixing the minimum of the reflected beam in zero (bottom panel of Fig. 7). In the next

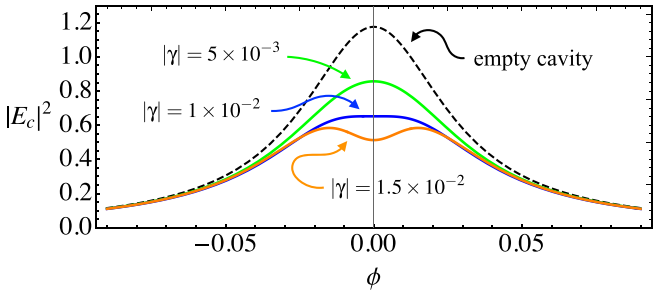

FIG. 5. Plots of the $|E_c|^2$ as a function of ϕ in the de-amplification regime ($\phi_p = \pi/2$) for different values of $|\gamma|$ as reported in the figure. The dashed line refers to the empty cavity. The other parameters involved have been set to the realistic values $R_1 = 0.999$, $R_2 = 0.9$, and $\Delta = 3.0 \times 10^{-3}$.

section (III) we show the experimental technique to achieve both goals.

III. EXPERIMENTAL SETUP AND RESULTS

The theory introduced in the previous section has been tested using the experimental setup depicted in Fig. 8. Our setup allows us to generate, manipulate and detect displaced squeezed states. We have control on both the amplitude and the phase of the state and also on the amplitude and phase of the pump. Following the scheme in Fig. 8, the setup consists of three main blocks. A homemade laser source (LASER) is a Nd:YAG and it generates both the seed (at 1064 nm) and the pump (at 532 nm, 320 mW for the results presented) for the OPO, since it is internally frequency doubled with a PPNL

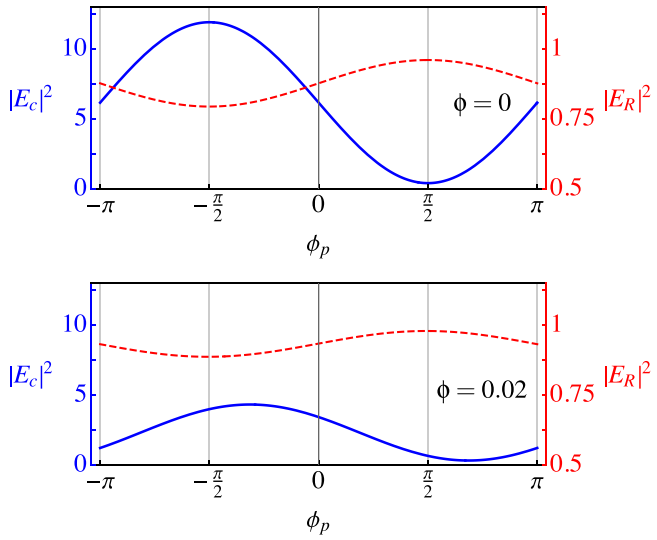

FIG. 6. Plots of $|E_c|^2$ (solid blue lines), proportional to the OPO output, and $|E_R|^2$ (dashed red lines) with $E_{in} = 1$ (dimensionless units) as functions of the phase ϕ_p for different values of $\phi \propto \nu$: (top) $\phi = 0$ (resonance), in this case $|E_R|^2$ corresponds to the minimum value of the reflected beam displayed in the bottom panel of Fig. 2; (bottom) $\phi = 0.02$. The other involved parameters have been set to the realistic values $R_1 = 0.999$, $R_2 = 0.9$, $\Delta = 3.0 \times 10^{-3}$, and $|\gamma| = 2.0 \times 10^{-2}$.

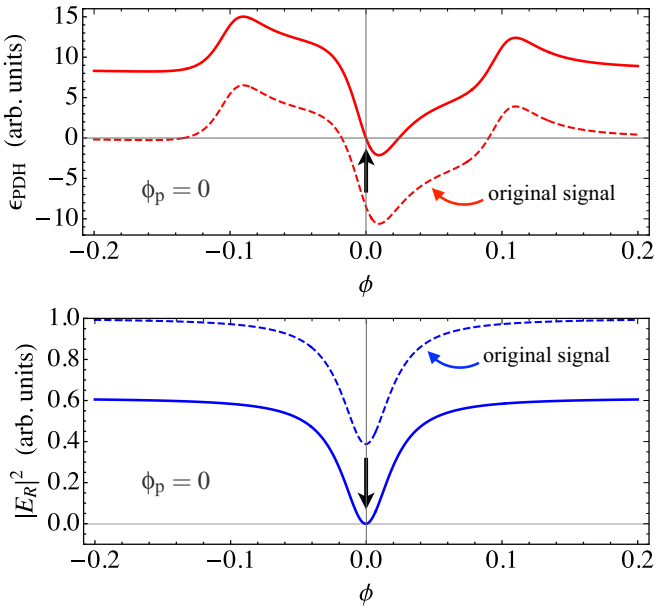

FIG. 7. Plots of the PDH error signal ϵ_{PDH} (top panel) and the amplitude of the reflected beam $|E_R|^2$ (bottom panel) as functions of $\phi \propto \nu$ for the pump phase $\phi_p = \pi$. The dashed lines refer to the original signals (see the center panel of Fig. 3 and the lower panel of Fig. 3), while the solid lines are obtained by setting to zero the ϵ_{PDH} offset and the minimum of $|E_R|^2$, respectively. The other involved parameters have been set to the realistic values $R_1 = 0.999$, $R_2 = 0.9$, $\Delta = 3.0 \times 10^{-3}$, and $|\gamma| = 2.0 \times 10^{-2}$.

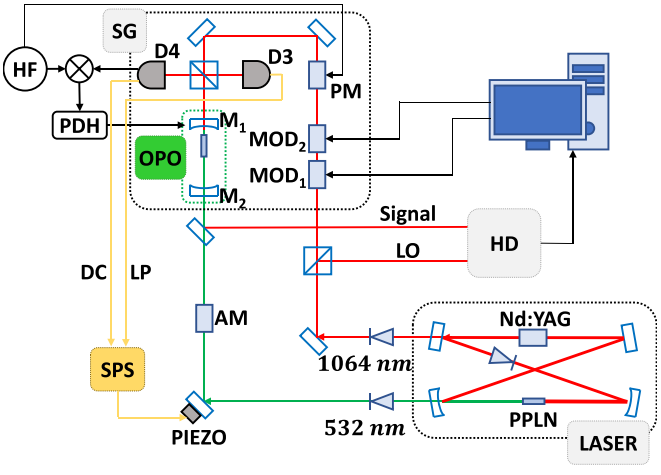

FIG. 8. Scheme of our setup. The main parts are three: a LASER which produces both the pump at 532 nm and the seed and the local oscillator (LO) at 1064 nm for the state detection; a state generation part (SG) used for quantum states generation and squeezing; a detection part based on homodyne detection (HD). An amplitude modulator (AM) is used to control the pump intensity. The OPO frequency is stabilized implementing the canonical PDH technique exploiting a high-frequency generator (HF) and a phase modulator (PM), while the seed-pump phase stabilization is performed by the seed-pump stabilizer (SPS) and it is based on our technique. See text for details.

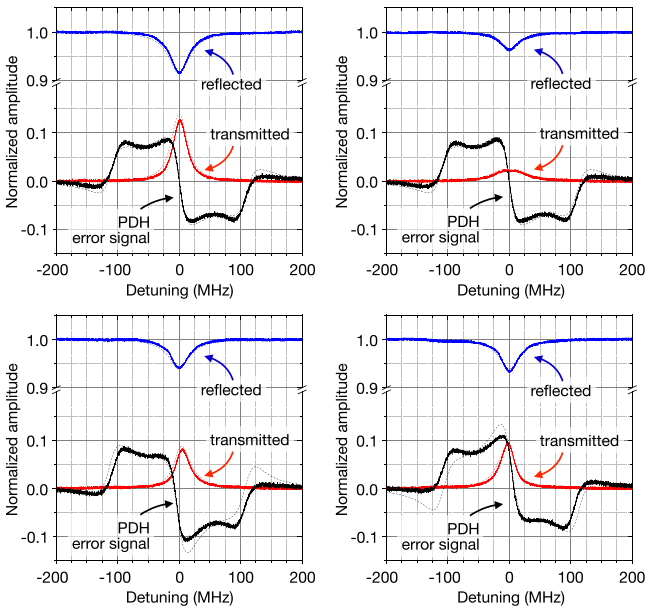

FIG. 9. Transmitted beam (lower red line), reflected beam (upper blue line) and PDH error signal (lower black line) as functions of the detuning ν, obtained with a frequency scan of the OPO cavity. Solid lines are experimental data, while dashed lines are theoretical trends obtained from R_1, R_2, Δ, and $|\gamma|$. We plot curves in the amplification regime ($\phi_p = -\pi/2$, upper left), de-amplification regime ($\phi_p = \pi/2$, upper right), *minus* regime ($\phi_p = 0$, lower left), and *plus* regime ($\phi_p = \pi$, lower right). For the theoretical previsions we used the following measured values of the experimental parameters $R_1 = 0.9988$, $R_2 = 0.917$, $\Delta = 2.4 \times 10^{-3}$, and $|\gamma| = 1.85 \times 10^{-2}$.

crystal. The internal second-harmonic generation has a major advantage: it behaves as a damping force which suppresses the laser relaxing oscillations, dramatically decreasing its noise. Therefore, this configuration avoids the necessity of building an external cavity for the second-harmonic generation and of introducing other elements for the noise suppression [18]. The second block, the state generation (SG), is composed of two modulators (MOD_1 and MOD_2), which create quantum states on 3 MHz sidebands, and an OPO used for squeezing. A 10-mm-long MgO:$LiNbO_3$ crystal with antireflection coating is placed inside the cavity. States are then detected with a conventional homodyne detection scheme (HD), the third block of the setup, where a fraction of the source laser serves as the local oscillator (LO).

Both generation and detection are controlled by a computer. The OPO is stabilized by using a standard PDH technique [8,17], while the pump phase stabilization is performed with our method (SPS) based on the theoretical considerations given in Sec. II. As shown in Fig. 8, the detector D3 monitors the laser amplitude fluctuations (LP), so that the SPS error signal (DC) can be compensated for them. This error signal is manipulated with a proportional-integral controller (PI) and applied to a piezoelectric which varies the pump path length, resulting in a change of its phase in the OPO. The laser has a free spectral range of 200 MHz, while OPO of 3025 MHz (cavity length 37 mm). Figure 9 shows the experimental intensity of the transmitted beam (red), of the reflected beam (blue), and of the PDH error signal

(black) as functions of the detuning ν, obtained with a scan of the OPO. The scan is performed by applying a linear voltage to a piezoelectric actuator attached to the output coupler of the OPO. The solid lines represent experimental data, while the dashed ones are the theoretical previsions. In the figure we consider four configurations with different relative seed-pump phases. The upper-left panel refers to the amplification regime, where $\phi_p = -\pi/2$: in this configuration the transmitted beam is maximum, the reflected beam is minimum, and the PDH error signal is zero when the OPO is resonant with the laser. The upper-right panel refers to the de-amplification regime, where $\phi_p = \pi/2$: as in the previous case, both the transmitted and the reflected beams are centered around the OPO resonance, i.e., $\phi = \nu = 0$, with ν being the detuning. Notice the two small relative maxima in the transmitted beam around the resonance, both in theoretical and in experimental curves (see also the center panel of Fig. 4). The lower-left and lower-right panels of Fig. 9 refer to two intermediate regimes that we call *minus*, where $\phi_p = 0$, and *plus*, respectively. We can clearly see that the PDH error signal has a negative (for $\phi_p = 0$) or positive ($\phi_p = \pi$) offset for the OPO resonance (see also the center panel of Fig. 3).

The experimental data are in very good agreement with the theoretical predictions obtained using the derived parameters of mirror reflectivities and nonlinear crystal losses, namely, $R_1 = 0.9988$, $R_2 = 0.917$, and $\Delta = 2.4 \times 10^{-3}$, that have been measured experimentally and are compatible with the values listed in the data sheet. Moreover, from the transmitted powers in amplification and de-amplification regimes we calculated $G = 5.68$ and, finally, we derived $|\gamma| = 1.85 \times 10^{-2}$ using Eq. (5). We stress that, in the two regimes, *minus* and *plus* the PDH error signal presents an offset in the resonance condition; that is, the error signal does not vanish at resonance. If we shift the PHD signal offset to zero with a suitable compensation, the PDH technique will allow us to stabilize the OPO cavity at resonance also with $\phi_p \neq \pm\pi/2$. Moreover, since the actual value of the minimum of the reflected beams is a monotonic function of the pump phase for $(2k-1)\pi/2 + k\pi < \phi_p < (2k+1)\pi/2$, $k \in \mathbb{Z}$, as one can see from Fig. 2, we can always set this minimum to zero in order to retrieve an error signal to stabilize the pump phase. This point will be better clarified in the following.

Figure 10 shows the amplitudes of the reflected and transmitted beams for a pump phase scan. A piezoelectric actuator is attached to a mirror used to change the pump phase ϕ_p and a linear voltage is applied. The OPO is actively stabilized during the scan, where we put the PDH error signal offset to zero. It is clear that the reflected beam has a maximum in the de-amplification regime and a minimum in the amplification regime, as expected. Thus, after the application of a proper offset, the reflected beam power is a good error signal and can be used to stabilize ϕ_p at any value but $\pm\pi/2$, where the derivative of the error signal vanishes.

The advantage of our technique is that both PDH error signal for OPO stabilization and SPS error signal for the pump phase stabilization are obtained from the same reflected beam. This allows us to not touch the transmitted beam, which cannot suffer power losses since it contains the squeezed state.

The procedure for the optimization of the two offsets (PDH and SPS) is rather simple. Once the phase of the pump is

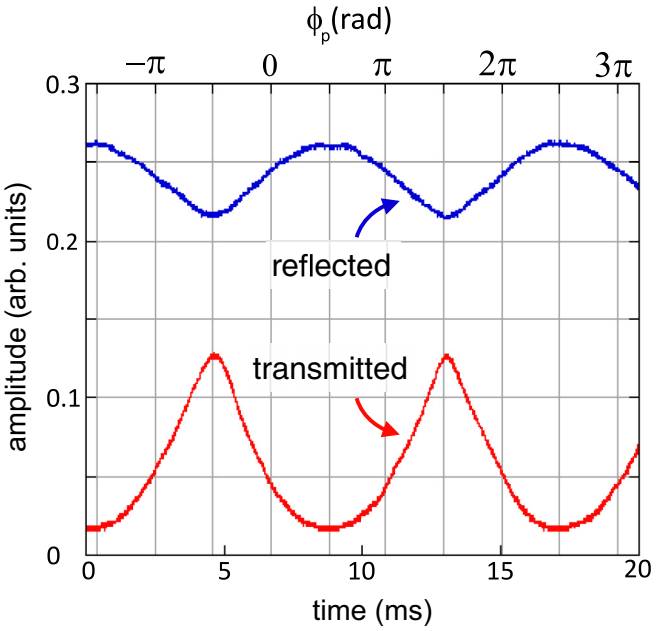

FIG. 10. Transmitted beam (lower red line) and reflected beam (upper blue line) for a scan of the cavity (here the time is related to the pump phase ϕ_p). A triangular signal has been applied to the PIEZO in Fig. 8 acting on the pump phase. For comparison with the theory, see the plots of $|E_R|^2$ and $|E_c|^2$ as functions of ϕ and ϕ_p in Figs. 2 and in 6, respectively.

chosen and, thus, the amplitude of the reflected beam at resonance, a scan of the OPO is performed and the two error signals mentioned above are monitored. An offset is added electronically to the PDH error signal in order to set it to zero where the reflected beam has its minimum, while another offset is added to the SPS error signal to shift to zero the value of the amplitude of the reflected beam at the same point (see also Fig. 7). Figure 11 shows the two experimental signals after this optimization in a configuration near the *minus* configuration. It is worth noting that the needed offset is added to the *values* of the signals not by physically acting on the optical setup, but by electronic means. To compensate the SPS error signal for the laser power fluctuations, we subtract the direct laser power from it. Finally, both the resulting SPS error signal and the PDH error signal are independently processed with two homemade PIs and applied to the piezoelectric actuator for changing ϕ_p and the cavity length, respectively. Figure 12 displays the amplitude of the transmitted beam of the OPO in three different cases. The red line refers to the condition without the pump and the relative power fluctuations are 0.6%. The black line refers to the *minus* condition ($\phi_p = 0$). Both the integrative and the proportional of the SPS PI are activated and the relative power fluctuations are 1.9%. Finally, the light blue line refers again to the *minus* condition, but now the proportional is switched off and the relative power fluctuations are 6.2%. In this last case the fluctuations have the typical frequency of the mountings mechanical vibrations, which is of the order of kHz. Black and blue curves have been rigidly shifted in the amplitude direction of -0.2 and -0.4, respectively, in order to better visualize them. It is worth noting that, once the OPO and the pump phase are stabilized, the system

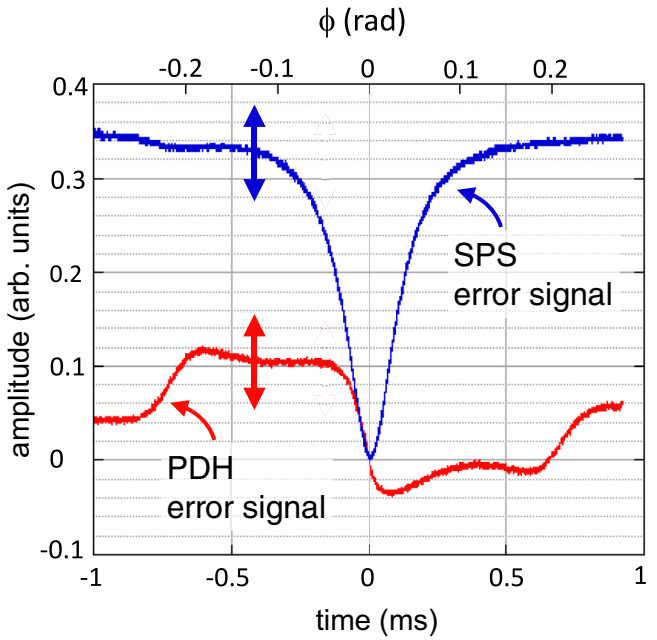

FIG. 11. PDH error signal (lower red line) and SPS error signal (upper blue line) during a scan of the cavity frequency with all the offsets optimized (here the time is related to the phase $\phi \propto \nu$). The two signals can be electronically shifted along the vertical axis, as highlighted by the arrows: we can set to zero the signals without physically affecting the optical setup.

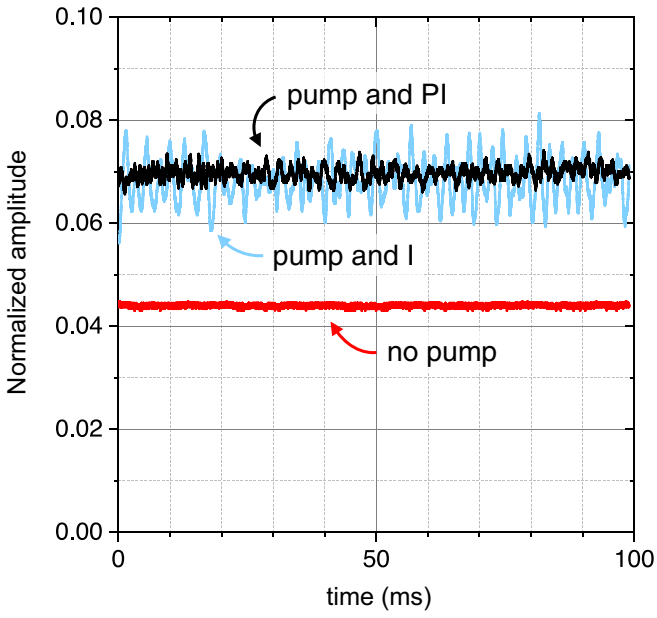

FIG. 12. Example of OPO stabilization in different conditions as a function of time. Lines represent the transmitted beam in three cases: (i) pump turned off (lower red line), (ii) pump on and pump phase stabilized at $\phi_p = 0$ with both integrator and proportional (upper black line), and (iii) pump on and pump phase stabilized at $\phi_p = 0$ with the only integrator (upper light blue line). The relative intensity noise is 0.6%, 1.9%, and 6.2%, respectively. Notice that the black line has been rigidly shifted of -0.4 for a better visualization.

remains stable for a long time, even hours. The only limiting factor is the dynamics of the two piezoelectric actuators, which can reach their maximum (or minimum) elongation if the thermal deformations are too large.

IV. APPLICATION: RELIABLE GENERATION OF DISPLACED SQUEEZED STATES

In this section we demonstrate the potentiality of our technique by applying the method to create displaced squeezed states. More precisely, taking into account the losses, the density operator describing the single-mode states we generate and analyze can be written in the following compact form [19,20]:

$$\rho = D(\alpha)S(\xi)\rho_{\rm th}S^\dagger(\xi)D^\dagger(\alpha), \tag{11}$$

where, as usual, $D(\alpha) = \exp(\alpha a^\dagger - \alpha^* a)$ and $S(\alpha) = \exp[\frac{1}{2}\xi a^2 - \frac{1}{2}\xi^*(a^\dagger)^2]$ are the displacement and squeezing operators, respectively, a being the annihilation operator of the field, $[a, a^\dagger] = \mathbb{I}$. In the previous formula we also introduced the density operator of the *thermal state*

$$\rho_{\rm th} = \sum_{n=0}^{\infty} \frac{(N_{\rm th})^n}{(1+N_{\rm th})^{n+1}} |n\rangle\langle n|. \tag{12}$$

We remark that the state (11) is the *overall* state generated by our setup [19,21]. In this context, the average number $N_{\rm th}$ of thermal photons can be seen as an effective parameter summarizing the effect of losses (only if $N_{\rm th} = 0$ we have no losses at all and the generated state is thus pure). For such a state the squeezing level in dB is given by $-10\log_{10}[(1+2N_{\rm th})e^{-2|\xi|}]$. For the sake of simplicity, but without loss of generality, we considered states with $\alpha \in \mathbb{R}$ and $\xi \in \mathbb{C}$ and we also obtain $\arg(\xi) = \phi_p + \pi/2$.

The addressed states have been generated through our setup following the well-established procedure described in Refs. [6,7,22,23]. Figure 13 shows the experimental homodyne traces of three examples of different states (left) and their tomographic reconstructions, represented in the phase space (right). In the plots it is clear the modulation of the quadrature standard deviation due to the squeezing (dashed lines in the left plots) as well as the relative phase between the coherent amplitude (set to zero) and the squeezing parameter ξ (related to the angle between the x_0 axis and the major axis of the ellipses in the right plots). The latter is indeed a proof of the reliability of our pump-seed phase stabilization technique, being the pump and seed phases connected to the squeezing parameter and coherent amplitude parameters.

We remark that, since the aim of our study was to demonstrate the effectiveness of the technique we developed, in our experiments we used a pump laser with a not very high intensity, thus resulting in a squeezing level around 3 dB, as shown in Fig. 13.

V. CONCLUSIONS

In this work we presented a theoretical model and experimental verification of a method for the stabilization of the relative phase between seed and pump of an OPO. To this aim, we have also developed a proper model of the OPO to obtain the analytical expression for the amplitude of the beam

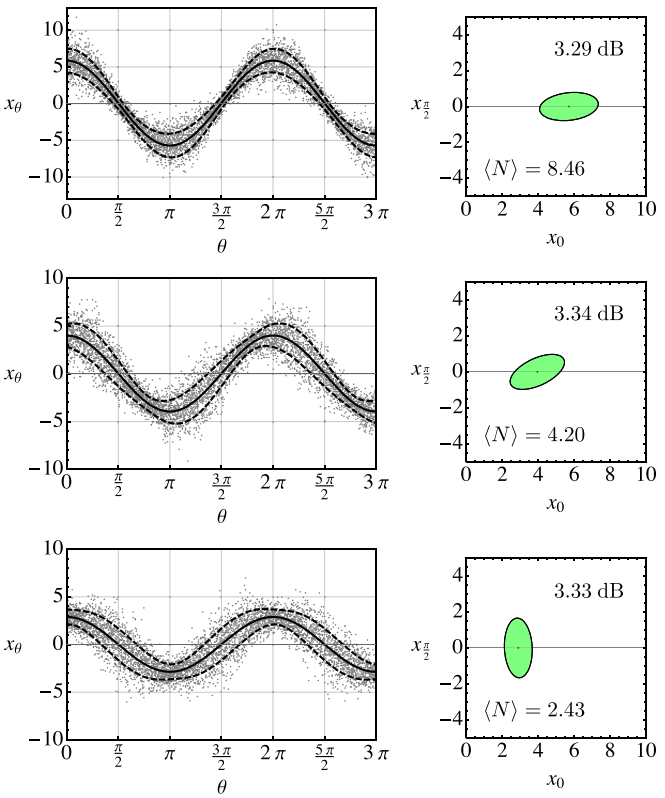

FIG. 13. Examples of displaced squeezed states generation with different homodyne traces (left plots) and the corresponding tomographic reconstruction in the phase space (right plots). (top) Amplification regime with $\phi_p \approx -\pi/2 \Rightarrow \arg(\xi) \approx 0$, $\alpha = 2.93$ and $N_{th} = 0.13$. (center) $\phi_p \approx 0 \Rightarrow \arg(\xi) \approx \pi/2$, $\alpha = 1.97$, and $N_{th} = 0.12$. (bottom) De-amplification regime $\phi_p \approx \pi/2 \Rightarrow \arg(\xi) \approx \pi$, $\alpha = 1.44$, and $N_{th} = 0.14$. In the left plots, the solid lines refer to the average value of the experimental trace, while the dashed lines represents the standard deviation, better highlighting the effect of squeezing. Note that, in the phase space (right plots), the angle between the major axis of the ellipses and the horizontal one is given by $\arg(\xi)/2$. In the pictures we also report the corresponding squeezing level and total average number of photons. The vacuum variance is set to 1.

reflected off the cavity as a function of the cavity frequency, of the crystal nonlinearity, and of the pump phase. In particular, our technique allows us to extract two error signals from the reflected beam, one for the stabilization of the pump-seed phase and one for the OPO frequency with the PDH technique, without the necessity of two different modulation and demodulation systems required by other methods (see, for instance, the Appendix). Our analysis shows that the pump affects the PDH error signal adding an offset that has to be compensated and that depends on the pump phase. We have also shown that our system allows the suppression of the noise caused by pump phase fluctuations to 1.9% on the transmitted beam, leading to an improvement of the squeezing level. Eventually, the reliability of our technique can pave the way not only for practical applications exploiting squeezed coherent states but also for studying more fundamental aspects of quantum information science based on continuous-variable systems.

ACKNOWLEDGMENTS

This work has been supported by MAECI, Project No. PGR06314 "ENYGMA."

APPENDIX: ALTERNATIVE METHOD FOR PUMP STABILIZATION

In this Appendix we present another method for the pump stabilization that is suggested in Ref. [12]: it is based on modulating the pump entering the OPO with sidebands. In this case the γ parameter can be written as

$$\gamma_m = \gamma - i\beta \sin(2\pi \nu_m t). \tag{A1}$$

The two sidebands of the pump stimulates the generation of two sidebands at frequency ν_m, which are not resonant with the OPO cavity. This leads to an error signal with three terms: the central term E_R and the two sidebands at frequency ν_m given by the transmitted part of E_R on the sidebands. Thus the error signal for this technique can be written as

$$\epsilon_B = \mathrm{Im}[E_R(\nu)E_m^*(\nu) - E_R^*(\nu)E_m(\nu)],$$

where the field E_m can be obtained from E_R in Eq. (7) by taking into account the contribution from $i\gamma(1 - R_1)$. Therefore, one has

$$E_m = i\gamma \frac{\sqrt{1-R_1}}{\sqrt{R_1}} E_c^*. \tag{A2}$$

It is clear that, in order to work, the present technique requires a modulation on the pump as well as a modulation on the seed for the PDH OPO stabilization. This last modulation has to be performed at a different frequency with respect to the pump modulation. For this reason, one needs two different modulation, demodulation and detection stages, which is a possible disadvantage.

[1] C. Weedbrook, S. Pirandola, R. García-Patrón, N. J. Cerf, T. C. Ralph, J. H. Shapiro, and S. Lloyd, Gaussian quantum information, Rev. Mod. Phys. **84**, 621 (2012).

[2] J. Lough, E. Schreiber, F. Bergamin, H. Grote, M. Mehmet, H. Vahlbruch, C. Affeldt, M. Brinkmann, A. Bisht, V. Kringel *et al.*, First Demonstration of 6 dB Quantum Noise Reduction in a Kilometer Scale Gravitational Wave Observatory, Phys. Rev. Lett. **126**, 041102 (2021).

[3] G. Breitenbach, S. Schiller, and J. Mlynek, Measurement of the quantum states of squeezed light, Nature (London) **387**, 471 (1997).

[4] V. D'Auria, S. Fornaro, A. Porzio, S. Solimeno, S. Olivares, and M. G. A. Paris, Full Characterization of Gaussian Bipartite Entangled States by a Single Homodyne Detector, Phys. Rev. Lett. **102**, 020502 (2009).

[5] D. Buono, G. Nocerino, V. D'Auria, A. Porzio, S. Olivares, and M. G. A. Paris, Quantum characterization of bipartite Gaussian states, J. Opt. Soc. Am. B **27**, A110 (2010).

[6] C. Porto, D. Rusca, S. Cialdi, A. Crespi, R. Osellame, D. Tamascelli, S. Olivares, and Matteo G. A. Paris, Detection of squeezed light with glass-integrated technology embedded into a homodyne detector setup, J. Opt. Soc. Am. B **35**, 1596 (2018).

[7] A. Mandarino, M. Bina, C. Porto, S. Cialdi, S. Olivares, and M. G. A. Paris, Assessing the significance of fidelity as a figure of merit in quantum state reconstruction of discrete and continuous-variable systems, Phys. Rev. A **93**, 062118 (2016).

[8] R. Drever, J. Hall, F. Kowalski, J. Hough, G. Ford, A. Munley, and H. Ward, Laser phase and frequency stabilization using an optical resonator, Appl. Phys. B: Photophys. Laser Chem. **31**, 97 (1983).

[9] M. Heurs, I. R. Petersen, M. R. James, and E. H. Huntington, Homodyne locking of a squeezer, Opt. Lett. **34**, 2465 (2009).

[10] T. Hansch, and B. Couillaud, Laser frequency stabilization by polarization spectroscopy of a reflecting reference cavity, Opt. Commun. **35**, 441 (1980).

[11] N. P. Robins, B. J. J. Slagmolen, D. A. Shaddock, J. D. Close, and M. B. Gray, Interferometric, modulation-free laser stabilization, Opt. Lett. **27**, 1905 (2002).

[12] W. P. Bowen, Ph.D. thesis, School of physical sciences, Australian National University, 2003.

[13] X. Sun, Y. Wang, L. Tian, S. Shi, Y. Zheng, and K. Peng, Dependence of the squeezing and anti-squeezing factors of bright squeezed light on the seed beam power and pump beam noise, Opt. Lett. **44**, 1789 (2019).

[14] H. Vahlbruch, S. Chelkowski, B. Hage, A. Franzen, K. Danzmann, and R. Schnabel, Coherent Control of Vacuum Squeezing in the Gravitational-Wave Detection Band, Phys. Rev. Lett. **97**, 011101 (2006).

[15] T. Denker, D. Schutte, M. H. Wimmer, T. A. Wheatley, E. H. Huntington, and M. Heurs Utilizing weak pump depletion to stabilize squeezed vacuum states, Opt. Express **23**, 16517 (2015).

[16] A. Yariv and P. Yeh, *Optical Waves in Crystals Propagation and Control of Laser Radiation* (Wiley-Interscience, New York, 2002).

[17] E. D. Black, An introduction to Pound–Drever–Hall laser frequency stabilization, Am. J. Phys. **69**, 79 (2001).

[18] S. Cialdi and E. Suerra (unpublished).

[19] S. Olivares, Quantum optics in the phase space, Eur. Phys. J. Spec. Top. **203**, 3 (2012).

[20] S. Olivares, Introduction to generation, manipulation and characterization of optical quantum states, Phys. Lett. A **418**, 127720 (2021).

[21] M. N. Notarnicola, M. G. Genoni, S. Cialdi, M. G. A. Paris, and S. Olivares, Phase noise mitigation by realistic optical parametric oscillator, arXiv:2106.11631.

[22] S. Cialdi, E. Suerra, S. Olivares, S. Capra, and M. G. A. Paris, Squeezing Phase Diffusion, Phys. Rev. Lett. **124**, 163601 (2020).

[23] S. Olivares, S. Cialdi, and M. G. A. Paris, Homodyning the $g^2(0)$ of Gaussian states, Opt. Commun. **426**, 547 (2018).